RECENT RESULTS FROM THE CRYSTAL BARREL EXPERIMENT AT ELSA

U. THOMA

HISKP, Bonn University
Nussallee 14 - 16
53115 Bonn, Germany
E-mail: thoma@hiskp.uni-bonn.de

Experiments with electromagnetic probes are promising to search for new baryon states and to determine the properties of baryon resonances. The Crystal Barrel experiment at ELSA is very well suited to investigate final states with neutral mesons decaying into photons. Interesting results on baryon resonances have been obtained. In particular a new $D_{15}(2070)$ decaying into $p\eta$ was recently observed. In multi-meson final states such as $p\pi^0\pi^0$ and $p\pi^0\eta$ baryon cascades occur. Baryon resonances decaying not only into $\Delta\pi$ but also into $D_{13}(1520)\pi$, $S_{11}(1535)\pi$, and via a higher mass state around 1660 MeV are observed.

1. Introduction

At medium energies, our present understanding of QCD is limited. Here, in the energy regime of meson and baryon resonances the strong coupling constant is large and perturbative methods can no longer be applied. One of the key issues in this energy regime is to identify the relevant degrees-of-freedom and the effective forces between them. A necessary step towards this aim is undoubtedly a precise knowledge of the experimental spectrum of baryon resonances and of their properties.

Quark models are in general amazingly successful in describing the spectrum of existing states. However, constituent quark models usually predict many more resonances than have been observed so far, especially at higher energies[1,2]. In addition the mass of some states are difficult to understand within a constituent quark model, such as e.g. the low mass of the $P_{11}(1440)$ or the $P_{33}(1600)$. Another example are the negative parity Δ^*-states around 1900 MeV, which at present still need experimental confirmation. An alternative description of the baryon spectrum in which baryon resonances are generated dynamically from their decays is devel-

oped in [3], evoking different degrees of freedom as the relevant ones.
Experiments need to provide a detailed knowledge on the spectrum but also of the properties of baryon resonances to test predictions from the different models and from lattice QCD-calculations. Experiments using electromagnetic probes, such as the Crystal Barrel experiment at ELSA, are not only able to search for unknown states but also to determine the properties of resonances like photo-couplings and partial widths. The properties of a resonance are also of big importance for an interpretation of its nature. One immediate debate is e.g. whether the $P_{11}(1440)$ is really a 3-quark state. A good understanding of production and decay properties may help to elucidate the nature of a state. In the following, different final states investigated with the Crystal Barrel detector at ELSA will be discussed.

2. The $\gamma p \to p\eta$-channel

New data on η-photoproduction has been taken by the CB-ELSA experiment in Bonn [4]. Due to its electromagnetic calorimeter consisting of 1380 CsI(Tl) crystals covering 98% of the 4π solid angle, the CB-ELSA detector is very well suited to measure photons. The η is observed either in its $\gamma\gamma$- or $3\pi^0$- decay. The two or six photons are detected in the calorimeter and the proton is identified in a 3-layer scintillating fiber detector. The invariant masses show a clear η signal over an almost negligible background (Fig. 1, top right). The differential and the total cross sections are shown in Fig. 1 in comparison to the TAPS[5], GRAAL[6] and CLAS[7] data. The new CB-ELSA data extends the covered angular and energy range significantly compared to previous measurements. The total cross section is obtained by integrating the differential cross sections. The extrapolation to forward and backward angles uses the result of the partial wave analysis (PWA) discussed below. The result of the PWA is shown as solid line Fig. 1. The formalism used in the PWA to extract the contributing resonances from the data is summarized in [15]. In the fit [10,17] the following following data sets were included in addition to the CB-ELSA data on $\gamma p \to p\eta$: The CB-ELSA data on $\gamma p \to p\pi^0$ [8], the TAPS data on $\gamma p \to p\eta$ [5], the beam asymmetries $\Sigma(\gamma p \to p\pi^0)$ and $\Sigma(\gamma p \to p\eta)$ from GRAAL[9], and $\Sigma(\gamma p \to p\pi^0)$, $\gamma p \to n\pi^+$ from SAID and data on $K\Lambda$ and $K\Sigma$ from SAPHIR[11,12], CLAS[13], and LEPS[14]. In the PWA a new state coupling strongly to the η-channel was found, an $D_{15}(2070)$ with a mass of $(2060 \pm 30)\,\mathrm{MeV}$ and a width of $(340 \pm 50)\,\mathrm{MeV}$. The χ^2-minimum of the overall fit is shown in Fig. 1. A clear minimum is observed. The $D_{15}(2070)$

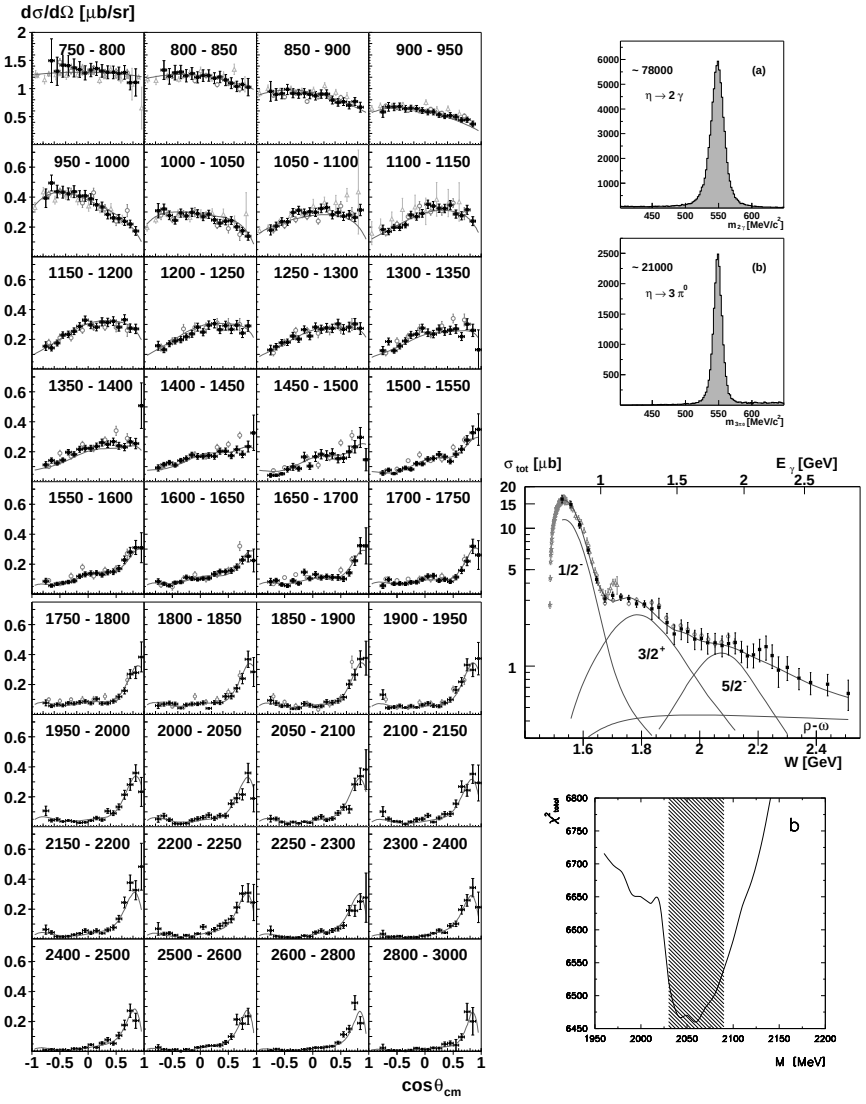

Figure 1. Left: Differential cross sections for $\gamma\,\mathrm{p} \to \mathrm{p}\,\eta$, for $E_\gamma = 750\,\mathrm{MeV}$ to $3000\,\mathrm{MeV}$: CB-ELSA(black squares)[4], TAPS[5], GRAAL[6] and CLAS[7] data (in light gray). The solid line represents the result of our fit. Right column: Invariant $\gamma\gamma$ and $3\pi^0$ invariant mass, total cross section (logarithmic scale) for the reaction $\gamma\,\mathrm{p} \to \mathrm{p}\,\eta$, χ^2 distribution for different masses of the D_{15} imposed in the fit. For further details see [10,4].

contributes rather strongly to the data set as shown in Fig.1. The PDB[16] includes a 2-star $D_{15}(2200)$. Its mass is rather badly determined and scatters from 1900 MeV to 2230 MeV the same is true for measurement of its width. Presently it is unclear whether all signals seen are due to the same state. Additional evidence for further new states found in the combined PWA is discussed in [10,17]. No evidence was found for a third S_{11} for which claims have been reported at masses of 1780 MeV [18] and 1846 MeV [19].

3. The $\gamma p \to p\pi^0\pi^0$-channel

At higher energies multi-meson final states play a role of increasing importance. Above 1900 MeV the spectrum and the properties of resonances are rather badly known, while this is, according to quark model predictions, the energy regime where many new states should occur. Predictions indicate that many of the so far unobserved states should have a significant $\Delta\pi$-coupling[1]. Within the different $\gamma p \to N2\pi$-channels the $\gamma p \to p\pi^0\pi^0$-channel is the one best suited to investigate the $\Delta\pi$ decay of baryon resonances. Compared to other isospin-channels, many non-resonant-"background" amplitudes do not contribute like the diffractive ρ-production or the Δ-Kroll-Rudermann term. In addition, the number of possible Born terms and t-channel processes is strongly reduced; π-exchange is e.g. not possible. This leads to a high sensitivity of the $\gamma p \to p\pi^0\pi^0$-channel on baryon resonances decaying into $\Delta\pi$. The $\gamma p \to p\pi^0\pi^0$ cross section as measured by TAPS[20] in the low energy range and by GRAAL[21] up to an incoming photon energy of about 1500 MeV is shown in Fig. 2; two peak-like structures are observed. The data has been interpreted within the Laget-[22] and Valencia model[23], resulting in very different interpretations. In the Valencia-model, which is limited to the low energy region, the $D_{13}(1520)$ decaying into $\Delta(1232)\pi$ dominates the lower energy peak, while in the Laget-model the $P_{11}(1440)$ decaying into σp is clearly the dominant contribution. This shows that even-though both models lead to a reasonable description of the total cross section their interpretation of the data is in disagreement. Recently data on $\gamma p \to p\pi^0\pi^0$ has also been taken by the CB-ELSA experiment in Bonn extending the covered photon energy range up the E_γ=3.0 GeV ($\sqrt{s}$=2.6 GeV). To investigate the reaction $\gamma p \to p\pi^0\pi^0$, events with 4 photons are selected. In Fig 3 the invariant $p\pi^0$-mass is shown for two $\sqrt{s}$-bins. At low $\sqrt{s}$ only a peak due to the $\Delta(1232)$ is observed, at higher energies additional structures become visible. In addition to the $\Delta(1232)$ contributions from the $D_{13}(1520)$, and a

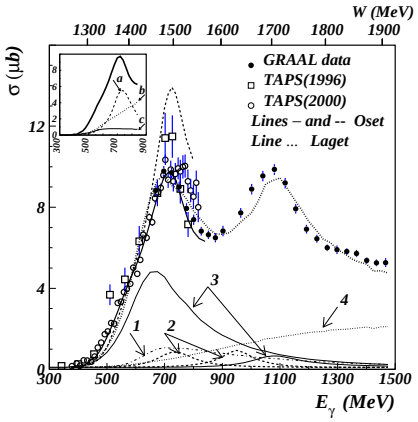

Figure 2. Total $\gamma p \to p2\pi^0$-photoproduction cross sections measured by GRAAL[21] and TAPS[20], shown together with the interpretation as given by Laget[22] and within the Valencia-model[23]. In the lower part if the figure the partial contributions as found in the Laget model are given: (1) $\gamma p \to P_{11}(1440) \to \Delta\pi$, (2) $\gamma p \to D_{13}(1520), D_{13}(1710) \to \Delta\pi$, (3) $\gamma p \to P_{11}(1440), P_{11}(1710) \to p\sigma$, (4) $\gamma p \to p\sigma$. In the inset the Valencia-model calculation is shown; lines (a), (b), (c) for $D_{13}(1520)$, Δ, and $P_{11}(1440)$ intermediate states, respectively. The figures are taken from[21].

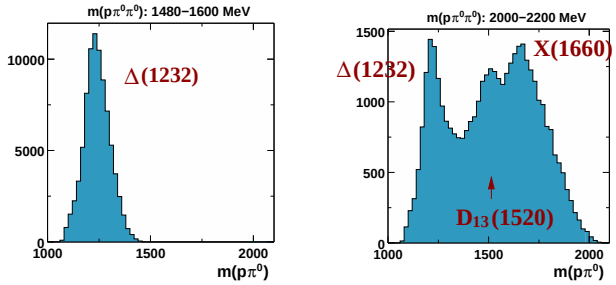

Figure 3. Left: $p\pi^0$ invariant mass for events with $\sqrt{s}$=1.48-1.6 GeV (left), and $\sqrt{s}$= 2.-2.2 GeV (right).

further state around 1660 MeV is observed. For further details on the data as well as for differential and total cross sections see [24]. To extract the contributing resonances, their quantum numbers and their properties from the data, a partial wave analysis (PWA) has been performed. The formalism used is summarized in [15]. For the parametrisation of s-channel resonances either Breit-Wigners or K-matrices are used. t-channel processes are described by the exchange of Regge-trajectories. In addition u-channel amplitudes and Born-terms are included. An event-based, unbinned maximum-likelihood fit was performed; it takes all the correlations between the five independent variables correctly into account. The fits include the prelim-

inary TAPS data[25] in the low energy region in addition to the CB-ELSA data. The latter was taken using two beam energy settings (E_{e^-}=1.4 GeV, 3.2 GeV). Resonances with different quantum numbers were introduced in various combinations allowing, so far, for the following decay modes: $\Delta(1232)\pi$, $N(\pi\pi)_s$, $P_{11}(1440)\pi$, $D_{13}(1520)\pi$ and $X(1660)\pi$. For a good description of the data resonances like e.g. the $P_{11}(1440)$, the $D_{13}(1520)$, the $D_{13}/D_{33}(1700)$, the $P_{13}(1720)$, the $F_{15}(1680)$ as well as several additional states and background amplitudes are needed. An example for the quality of the data description reached is shown in Fig. 4. One preliminary result of the PWA is a dominant contribution of the $D_{13}(1520) \rightarrow \Delta\pi$ amplitude in the energy range where the first peak in the cross section occurs. Fig. 5 shows the $p\pi^0$ invariant mass and angular distributions in the $\sqrt{s}$-range from 1450 MeV to 1550 MeV. The $\Delta(1232)$ clearly dominates the $p\pi^0$ invariant mass. The PWA attributes most of these events to the $\gamma p \rightarrow D_{13}(1520) \rightarrow \Delta\pi$ amplitude. This interpretation gets further substantiated by looking at the angular distributions. The angular distribution for the $D_{13}(1520) \rightarrow \Delta\pi$-amplitude has a very similar shape as the data. This is not the case for the $P_{11}(1440)$. The preliminary result of our analysis is therefore in contradiction to the interpretation given within the Laget model, where the $P_{11}(1440) \rightarrow p\sigma$-amplitude dominates in this energy range. Another result of the PWA is the observation of baryon cascades. Baryon resonances not only decaying into $\Delta\pi$ but also via $D_{13}(1520)\pi$ and $X(1660)\pi$ are observed for the first time. The according enhancements are already visible in the corresponding $p\pi^0$ invariant

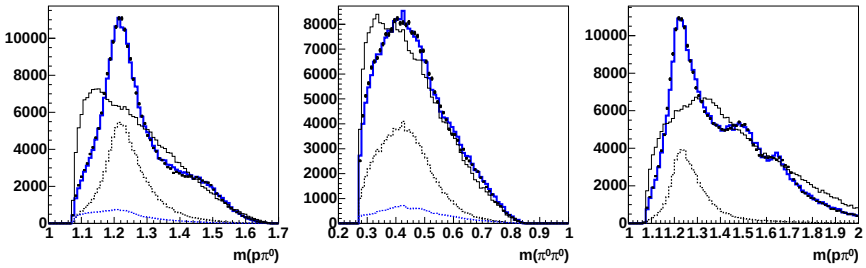

Figure 4. Invariant mass distributions in comparison to the PWA-result for the lower energy CB-ELSA data (without acceptance correction). Each plot shows the experimental data (points with error bars), and the result of the PWA (solid gray curve). The contribution of the $D_{13}(1520)$ and the $P_{11}(1440)$ are shown as dashed black (upper) and dashed gray (lower) curves, respectively. The thin black line represents the phase space distribution. The description of the angular distributions are of similar quality. Right: $p\pi^0$ invariant mass for the higher energy data set (E_γ=0.8-3.0 GeV) in comparison to the result of the PWA. (preliminary)

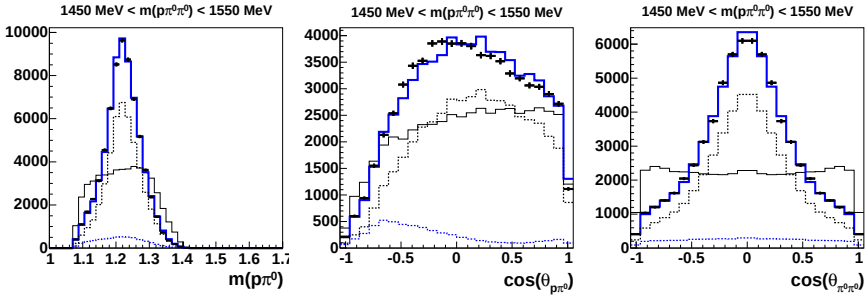

Figure 5. $p\pi^0$ invariant mass and angular distributions for $\sqrt{s}$=1450-1550MeV. See Figure 4 for the meaning of the different curves.

mass (Fig. 3). The observation of baryon cascades is also interesting in respect to the search for states which might not couple to πN and γp; they still could be produced in such baryon cascades. Presently, a combined analysis of this data together with the single meson photoproduction data discussed in Section 2 and the Crystal Ball data on $\pi^- p \to n\pi^0\pi^0$ [26] is in progress.

Recently the result of the $\gamma p \to p\pi^0\pi^0$ double polarization experiment performed by the GDH-collaboration at MAMI has been published [27]. It was found that the $\sigma_{3/2}$ component which cannot be due to the $P_{11}(1440)$ dominates in the energy region up to about 800 MeV. According to the Valencia-model[23,28] the $D_{13}(1520)$-resonance is largely responsible for the observed dominance of the $\sigma_{3/2}$ cross section. The non-negligible $\sigma_{1/2}$ component observed is presently underestminated by the Valencia-model (Fig. 6, left). Using the result of our PWA obtained by fitting the unpolarized data only, $\sigma_{3/2}$ and $\sigma_{1/2}$ have been calculated. Our result in comparison to the data is shown in Fig. 6, right. A nice agreement between our fit result and the data is observed.

4. The $\gamma p \to p\pi^0\eta$-channel

The $p\pi^0\eta$-final state is another interesting final state. Here, e.g., the decay of Δ^* resonances into $\Delta\eta$ can be investigated. This decay has the advantage of being isospin selective; no N^* resonances can be produced.

This reaction is e.g. well suited to investigate the existence of the negative parity Δ^*-states around 1900 MeV. These states would, if they exist, pose a problem for quark model calculations because of their low mass. But so far the evidence for their existence is weak. Only one of the three states, $S_{31}(1900)$, $D_{33}(1940)$, and $D_{35}(1930)$ is a 3-star resonance, the $D_{35}(1930)$. The 1-star $D_{33}(1940)$ resonance can decay with orbital angular momentum

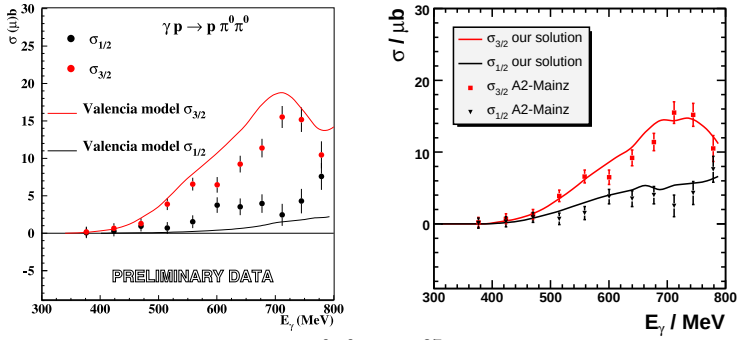

Figure 6. $\sigma_{3/2}$, $\sigma_{1/2}$ for $\gamma p \to p\pi^0\pi^0$ from [27] in comparison to the result obtained within the Valencia model (left) and calculated from our PWA-result determined by fitting the unpolarized data only (right).

zero into $\Delta\eta$, which makes the $p\pi^0\eta$-final state a good place to investigate the existence of this resonance.

With the Crystal Barrel detector at ELSA this final state has been investigated from threshold up to photon energies of 3.0 GeV. The $p\pi^0$ invariant mass (Fig. 7) shows that the data set is indeed dominated by $\Delta\eta$ events. In addition to the $\Delta(1232)$ there are other interesting structures observed, such as the $a_0(980)$ in the $\pi^0\eta$ invariant mass or the $S_{11}(1535)$ in the Dalitz plot. To extract the resonance contributions from the data a PWA of the $p\pi^0\eta$-final state has been performed. Three ambiguous solutions were found. All three result in a similar likelihood being based at the same time on quite different sets of contributing amplitudes. All three solutions do need a $D_{33}(\sim 1900)$ and show indications baryon cascades, e.g. decays of higher mass resonances not only via $\Delta\eta$ but also via $S_{11}(1535)\pi$. In addition there seem to be hints for a new higher mass resonance. But based on ambiguous solutions it is of course impossible to make a more definite

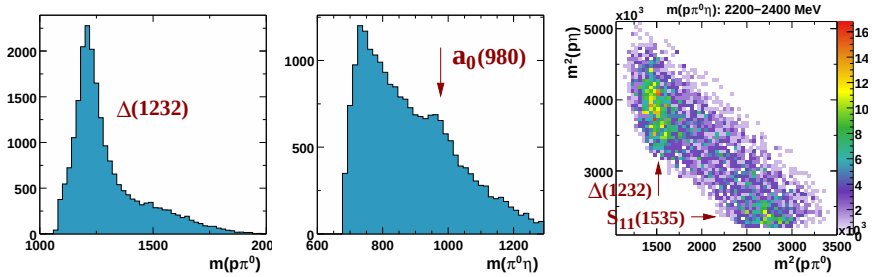

Figure 7. $\gamma p \to p\pi^0\eta$-events: $p\pi^0$ (left) and $\pi^0\eta$ (middle) invariant mass for $E_\gamma = E_{\text{threshold}} - 3.0$ GeV. Right: Dalitz plot for $\sqrt{s}$= 2.2-2.4 GeV.

statement. Further constraints are clearly needed.

5. Polarization measurements with Crystal Barrel at ELSA

The existence of ambiguous solutions in the PWA especially at higher energies shows clearly the need for polarization experiments.
A first step in this direction has been made with the CB-ELSA/TAPS setup at ELSA, where measurements using linearly polarized photons have been performed. For this data taking period 90 CsI(Tl) crystals have been removed in forward direction to open up a forward region $\pm 30^\circ$ which was then covered by the TAPS detector consisting out of 528 BaF_2 crystals. The analysis of this data to determine the beam asymmetries of various final states is presently in progress.
Presently the experimental setup at ELSA is modified for the new double polarization experiments. New forward detector components are installed. The measurements will use circularly or linearly polarized photons together with the Bonn frozen spin target [29], providing longitudinally polarized protons. The availability of a polarized beam and a polarized target gives access to various double and also single polarization observables, providing additional constraints for the PWA.
An example for the sensitivity of such double polarization measurements is shown in Fig. 8. Here, the quantum numbers of the new $D_{15}(2070)$ have been tested. $J^P = 5/2^-$ has been replaced in the fit by $1/2^+$ and $1/2^-$, respectively and the available data (see Section 2) has been refitted. While the differences in each of the differential cross sections are small, even though they add up to a significant change in χ^2, the differences in the calculated helicity differences from the three solutions are substantial (Fig. 8). This shows that with the new double polarization experiments we should not only be able to prove the existence of the new $D_{15}(2070)$ but also to confirm its quantum numbers. For a more detailed discussion on the polarization program see [30].

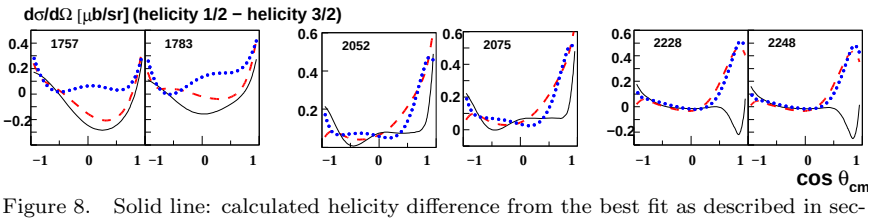

Figure 8. Solid line: calculated helicity difference from the best fit as described in section 2, dashed line: D_{15} quantum numbers replaced by $1/2^-$, dotted line: D_{15} quantum numbers replaced by $1/2^+$, the numbers in the picture indicate $\sqrt{s}$.

Acknowledgments

This work is supported by the Deutsche Forschungsgemeinschaft (DFG) within the SFB/TR16. The author acknowledges an Emmy Noether grant from the DFG.

References

1. S. Capstick and W. Roberts, Phys. Rev. **D47**, 1994 (1993), Phys. Rev. **D49**, 4570 (1994), S. Capstick, Phys. Rev. **D46**, 2864 (1992)
2. U. Loring, B. C. Metsch and H. R. Petry, Eur. Phys. J. A **10**, 395 (2001)
3. M.Lutz, this conference
4. V. Crede *et al.* [CB-ELSA Collab.], Phys. Rev. Lett. **94**, 012004 (2005)
5. B. Krusche *et al.*, Phys. Rev. Lett. **74**, 3736 (1995).
6. F. Renard *et al.* [GRAAL Collab.], Phys. Lett. B **528**, 215 (2002).
7. M. Dugger *et al.* [CLAS Collab.], Phys. Rev. Lett. **89**, 222002 (2002).
8. O. Bartholomy *et al.* [CB-ELSA Collab.], Phys. Rev. Lett. **94**, 012003 (2005)
9. J. Ajaka *et al.* [GRAAL collaboration], Phys. Rev. Lett. **81**, 1797 (1998), O. Bartalini *et al.* submitted to Eur. Phys. J. A.
10. A. V. Anisovich, A. Sarantsev, O. Bartholomy, E. Klempt, V. A. Nikonov and U. Thoma, Eur. Phys. J. A **25**, 427 (2005)
11. K. H. Glander *et al.*, Eur. Phys. J. A **19**, 251 (2004)
12. R. Lawall *et al.*, Eur. Phys. J. A **24**, 275 (2005)
13. J. W. C. McNabb *et al.* [The CLAS Collab.], Phys. Rev. C **69**, 042201 (2004)
14. R. G. T. Zegers *et al.* [LEPS Collab.], Phys. Rev. Lett. **91**, 092001 (2003)
15. A. Anisovich, E. Klempt, A. Sarantsev and U. Thoma, Eur. Phys. J. A **24**, 111 (2005)
16. S. Eidelman *et al.* [Particle Data Group], Phys. Lett. B **592** (2004) 1.
17. A. V. Sarantsev, V. A. Nikonov, A. V. Anisovich, E. Klempt and U. Thoma, Eur. Phys. J. A **25**, 441 (2005)
18. B. Saghai and Z. Li, Proceedings of NSTAR 2002, nucl-th/0305004.
19. G. Y. Chen, S. Kamalov, S. N. Yang, D. Drechsel and L. Tiator,
20. M. Wolf *et al.*, Eur. Phys. J. **A9**, 5 (2000). F. Härter *et al.*, Phys. Lett. **B401**, 229 (1997).
21. Y. Assafiri *et al.*, Phys. Rev. Lett. **90**, 222001 (2003).
22. J.-M. Laget, L. Y. Murphy, shown in [21].
23. J. A. Gomez Tejedor *et al.*, Nucl. Phys. **A600**, 413 (1996).
24. M. Fuchs, this conference
25. M. Kotulla, private communication.
26. S. Prakhov *et al.* [Crystal Ball Collab.], Phys. Rev. C **69**, 045202 (2004).
27. J. Ahrens *et al.* [GDH and A2 Collab.], Phys. Lett. B **624**, 173 (2005), H.-J. Arends, talk at NSTAR 2004.
28. J. Nacher *et al.*, Nucl. Phys. **A695**, 295 (2001), **A697**, 372 (2002).
29. Ch. Bradtke *et al.*, Nucl. Instr. and Meth. **A436**, 430 (1999).
30. H. Schmieden, this conference